[CANCER RESEARCH 62, 1057–1062, February 15, 2002]

WK175, a Novel Antitumor Agent, Decreases the Intracellular Nicotinamide Adenine Dinucleotide Concentration and Induces the Apoptotic Cascade in Human Leukemia Cells

Katja Wosikowski,[1] Karin Mattern,[2] Isabel Schemainda, Max Hasmann, Benno Rattel,[3] and Roland Löser

Pharmacology Department, Klinge Pharma, 81673 Munich, Germany

ABSTRACT

We recently developed a class of novel antitumor agents that elicit a potent growth-inhibitory response in many tumor cells cultured *in vitro*. WK175, a member of this class, was chosen as a model compound that showed strong *in vitro* efficacy. WK175 interferes with the intracellular steady-state level of NAD^+, resulting in a decreased cellular NAD^+ concentration. We found that WK175 induces apoptotic cell death without any DNA-damaging effect. The apoptotic death signaling pathway initiated by WK175 was examined in detail: mitochondrial membrane potential, cytochrome *c* release, caspase 3 activation, caspase 3 and poly(ADP-ribose) polymerase cleavage, and the appearance of a sub-G_1 cell cycle population were determined in time course studies in THP-1 (a human monocytic leukemia cell line) cells. We found activation of this cascade after 24 h of treatment with 10 nM WK175. Induction of apoptosis was prevented by bongkrekic acid, Z-Asp-Glu-Val-Asp-fluoromethylketone, and Z-Leu-Glu-His-Asp-fluoromethylketone, inhibitors of the mitochondrial permeability transition and of caspase 3 and 9, respectively, but not by Ac-Tyr-Val-Ala-Asp-CHO, a specific caspase 1 inhibitor, suggesting the involvement of the permeability transition pore, caspase 3, and caspase 9 in the WK175-induced apoptotic cascade. These results imply that decreased NAD^+ concentration initiates the apoptotic cascade, resulting in the antitumor effect of WK175.

INTRODUCTION

Apoptosis is the physiological mechanism via which aged, damaged, or mutated cells are removed from the organism throughout normal life. In addition, apoptosis constitutes the fate of proliferating cells whose death is induced by external agents, including conventional cancer chemotherapy (1–3). However, many conventional chemotherapeutic agents possess DNA-damaging effects, which can lead to genomic instability and the generation of resistant tumor phenotypes. To find a novel antitumor agent with a new mechanism of action was the goal of our investigations. WK175 is such a compound, with distinct characteristics of conventional chemotherapeutics. WK175 induced no DNA damage as tested in two different mutagenicity tests (Ames test and chromosomal aberration) and no p53 or p21 expression,[4] but it did induce delayed cell death. WK175-induced apoptosis is not associated with activation of ligand/receptor systems such as Fas/CD95, but WK175 interferes with the NAD^+ biosynthesis of the cells, which results in a decreased cellular NAD^+ content. In this study, the apoptosis-activating effect of WK175 is presented.

It is currently assumed that the apoptotic process can be divided into at least three functionally distinct phases (1, 4). During the induction phase, cells receive the death-inducing stimulus, such as receptor ligation, DNA-damaging agents, or radiation, and inhibitors of mitochondrial metabolism. The effector phase is characterized by events that are subject to regulatory mechanisms, whereas the degradation phase is beyond the point of no return in which catabolic enzymes become activated in an irreversible fashion. The induction phase of the apoptotic pathway is initiated by WK175 through the inhibitory effect on the pyridine nucleotide biosynthesis, resulting in decreased cellular NAD^+ levels.

Alterations of mitochondrial functions have been described as being important in the effector phase of the apoptotic process (5). It has been established that the opening of pores (PTPs)[5] of the mitochondrial membrane allows the free distribution of solutes with $M_r < 1500$, thereby leading to the immediate dissipation of the mitochondrial membrane potential ($\Delta\Psi_m$; Ref. 6). Opening of the PTPs causes the release of apoptogenic proteins such as AIF, cytochrome *c*, and Smac from the mitochondria into the cytosol (1, 7–9). These apoptogenic proteins are present in the intermembrane space of mitochondria (10). AIF is a nuclear-encoded intermembrane flavoprotein that translocates to the nucleus, where it induces caspase-independent peripheral chromatin condensation and degradation of DNA (11). In the cytosol, cytochrome *c* controls the assembly of an apoptosome, a large complex composed of an oligomer of Apaf-1 and pro-caspase 9 (12, 13). The formation of this complex results in activation of caspase 9 (10, 12). Activated caspase 9 subsequently cleaves and activates other caspases (14). Smac eliminates the inhibitory effect of inhibitors of apoptosis on caspases. Inhibitors of apoptosis suppress apoptosis by preventing the activation of pro-caspases and inhibiting the enzymatic activity of mature caspases. The activation of the caspases and subsequent events in the apoptotic cascade constitute the degradation phase of the apoptotic process. The activated caspases cleave a variety of target proteins, thereby disabling important cellular processes and breaking down structural components of the cell (3, 15, 16). The targets of such cleavage events include PARP (17). In addition, activated caspases lead to the cleavage of the inhibitor of caspase-activated DNase, resulting in the activation of caspase-activated DNase (15).

In this study, the induction, effector, and degradation phase of the apoptotic cascade induced by WK175 will be described. We found that WK175 induces decreased intracellular NAD^+ levels, leading to disruption of the mitochondrial membrane potential, release of cytochrome *c* from the mitochondria, activation of caspase 3, cleavage of caspase 3 and PARP, and DNA degradation.

MATERIALS AND METHODS

Cell Culture. THP-1 (human acute monocytic leukemia; ATCC TIB 202) cells were grown as suspension cultures in RPMI 1640 (Sigma Chemical Co.,

Received 9/4/01; accepted 12/17/01.

The costs of publication of this article were defrayed in part by the payment of page charges. This article must therefore be hereby marked *advertisement* in accordance with 18 U.S.C. Section 1734 solely to indicate this fact.

[1] To whom requests for reprints should be addressed. Present address: Wilex AG, Grillparzerstrasse 10, 81675 Munich, Germany. Phone: 49-89-41313866; Fax: 49-89-41313899; E-mail: katja.wosikowski@wilex.de.

[2] Present address: Institute of Hematology, Erasmus University Rotterdam, P. O. Box 1738, 3000 DR Rotterdam, the Netherlands.

[3] Present address: GPC Biotech AG, Frauenhoferstrasse 20, 82152 Martinsried/Munich, Germany.

[4] Unpublished results

[5] The abbreviations used are: PTP, permeability transition pore; PARP, poly(ADP-ribose) polymerase; AIF, apoptosis-inducing factor; PMSF, phenylmethylsulfonyl fluoride; DEVD-AFC, *N*-acetyl-Asp-Glu-Val-Asp-7-amino-4-trifluoromethylcoumarin; DAPI, 4′,6-diamidino-2-phenylindole; PBG, 0.5% (w/v) BSA, 0.1% (w/v) gelatin in PBS; ANT, adenine nucleotide transporter; VDAC, voltage-dependent anion channel; Z-DEVD-FMK, Z-Asp-Glu-Val-Asp-fluoromethylketone; Z-LEHD-TMK, Z-Leu-Glu-His-Asp-fluoromethylketone; Ac-YVAD-CHO, Ac-Tyr-Val-Ala-Asp-CHO.

Deisenhofen, Germany) supplemented with 10% FCS (Pan Systems, Aidenbach, Germany), 2 mM Glutamax I (Life Technologies, Inc., Paisly, United Kingdom), 100 units/ml penicillin, and 100 μg/ml streptomycin (Sigma Chemical Co.) in a humidified atmosphere containing 5% CO_2 at 37°C. During culture, the cell density did not exceed 1×10^6 cells/ml. To induce apoptosis, WK175 (Klinge Pharma, Munich, Germany) was added from a 1000× stock solution in ethanol or DMSO to the culture medium. All other reagents, unless indicated otherwise, were obtained from Sigma Chemical Co.

Cellular Metabolic Activity Assay. THP-1 cells were plated in 96-well plates (20,000 cells/well) and incubated with WK175. After 4 days, the WST-1 assay was performed according to the manufacturer's recommendations (Roche Diagnostics, Mannheim, Germany).

Determination of Intracellular Content of Pyridine Nucleotides. THP-1 cells were treated with 10^{-8} M WK175. For the determination of NAD^+ and $NADP^+$, acid extracts were prepared: 10^6 cells were washed in 0.9% NaCl, resuspended in 200 μl of ice-cold 0.5 M $HClO_4$, and incubated on ice for 15 min. The acid extracts were neutralized by adding 61 μl of 2 M KOH/0.2 M K_xPO_4 (pH 7.5) and then centrifuged at 13,000 × *g* for 3 min. For the determination of NADH and NADPH, the cell pellets were extracted with 200 μl of 0.02 N NaOH containing 0.5 mM L-cysteine. After 10 min at 60°C, the alkaline extracts were neutralized with 60 μl of 0.25 M Gly-Gly buffer (pH 7.6) and centrifuged. The supernatants were stored at −70°C. NAD(H) and NADP(H) were assayed using spectrophotometric enzymatic cycling techniques (modifications of the methods described by Pinder *et al.*; Ref. 18). NAD^+ and NADH were analyzed in a reaction solution of 150 μl, consisting of 1.8 mM WST-1, 70 μM 1-methoxy-5-methyl-phenazinium methyl sulfate, 20 IU alcohol dehydrogenase, 64 mM nicotinamide, and 0.32 M ethanol in 64 mM Gly-Gly buffer (pH 7.4). The reaction solution for the analysis of $NADP^+$ and NADPH contained 1.8 mM WST-1, 70 μM 1-methoxy-5-methyl-phenazinium methyl sulfate, 0.45 IU glucose-6-phosphate dehydrogenase, and 5 mM glucose-6-phosphate in 50 mM Tris buffer (pH 8.0). The reactions were started by adding the reaction solutions to 10 μl of cell extract or 10 μl of NAD^+/$NADP^+$ standard dilutions. After incubation for 15–30 min at 37°C, the absorbance was measured at 450 nm. Blanks without NAD^+ and $NADP^+$ were measured to correct for background activity. Samples were assayed in quadruplicate. The lowest content of NAD(H) and NADP(H) detectable in these assays was 5 pmol/10^6 cells.

Cytofluorometric Analysis of Mitochondrial Membrane Potential. To evaluate mitochondrial membrane potential ($\Delta\Psi_m$), cells were incubated with the $\Delta\Psi_m$-sensitive dye JC-1 (250 ng/ml; Molecular Probes Europe, Leiden, the Netherlands) for 20 min at 37°C, followed by analysis with a particle analyzing system (PAS; Partec, Münster, Germany). Data were analyzed using WinList software (Verity Software House, Topsham, ME).

Caspase 3 Activity Assay. Cells were collected and washed twice with PBS. Cells were resuspended in lysis buffer (ApoAlert CPP32 Assay Kit; Clontech, Palo Alto, CA) and extracted for 10 min on ice. Insoluble material was pelleted at 13,000 × *g*.

For the assay, 50 μl of lysate were diluted in 450 μl of cold protease buffer [10 mM HEPES/KOH (pH 7.5), 2 mM EDTA, 5 mM DTT, 1 mM PMSF, 10 μg/ml leupeptin, and 10 μg/ml aprotinin]. Substrate was added to obtain a final concentration of 50 μM DEVD-AFC (Biomol, Plymouth Meeting, PA). Fluorescent AFC production was measured at an excitation of 400 nm and an emission of 505 nm.

Preparation of Mitochondrial and Cytosolic Fractions. Cells were resuspended at 4×10^7 cells/ml in homogenization buffer [20 mM HEPES/KOH (pH 7.5), 250 mM sucrose, 10 mM KCl, 2 m $MgCl_2$, 1 mM EDTA, 1 mM DTT, 1 mM PMSF, 10 μg/ml leupeptin, and 10 μg/ml aprotinin] and disrupted using a Potter homogenizer with a Teflon pestle (20 strokes at 1,000 rpm). The homogenate was centrifuged twice to remove the nuclei (750 × *g* for 5 min at 4°C). The supernatant was fractionated into mitochondria and cytosol by centrifugation at 13,000 × *g* for 20 min.

Preparation of Cell Lysate for Immunoblot Analysis. Cells (4×10^5 cells/ml) were suspended in medium containing 10 nM WK175 and incubated for the indicated amount of days. Cells were lysed by adding 500 μl of lysis buffer [10 mM Tris-HCl (pH 7.6), 1 mM EDTA, 50 mM NaCl, 0.5% deoxycholate, 0.5% NP40, and 0.5% SDS] supplemented with 20 μg/ml aprotinin, 20 μg/ml leupeptin, 1 μM PMSF, and 50 units/ml DNase. The cell lysate was heated, and protein concentrations were determined with the BCA Protein Assay Kit (Pierce).

Immunoblot Analysis. For cytochrome *c* and cytochrome oxidase analysis, 5 μg of mitochondrial proteins and 25 μg of cytosolic proteins were separated by 15% SDS-PAGE and transferred to polyvinylidene fluoride membranes (Immobilon-P; Millipore, Bedford, MA). Blots were blocked with 3% nonfat dry milk in TTBS [20 mM Tris-HCl (pH 7.6), 155 mM NaCl, and 0.05% Tween 20] and probed with mouse anti-cytochrome *c* (denatured) antibody (Research Diagnostic, Flanders, NY) and mouse anti-cytochrome oxidase subunit I antibody (Molecular Probes), followed by alkaline phosphatase-conjugated goat antimouse antibody (Tropix, Bedford, MA). Blots were developed by chemiluminescence (Western Star Kit; Tropix) and detected using a charge-coupled device camera.

For analysis of caspase 3 and PARP cleavage, 30–54 μg of total protein extracts were fractionated by SDS-PAGE and immunodetected as described above. Blots were probed with mouse anti-caspase 3 antibody (Transduction Laboratories, Dianova, Hamburg, Germany) or rabbit anti-PARP (Roche Diagnostica).

Immunofluorescent Labeling. Cells were collected and washed with PBS. After fixation with 2% formaldehyde, cells were transferred to coverslips by cytospin (Shandon, Pittsburgh, PA) and subsequently permeabilized for 10 min in 0.5% Triton X-100 in PBS. They were then incubated for 10 min in 100 mM glycine in PBS, and DNA was stained by 1 μg/ml DAPI (Partec) in PBS and washed twice for 5 min with PBG. Incubation with the mouse anti-cytochrome *c* (native) antibody (Research Diagnostic) was performed for 1–2 h at room temperature after dilution in PBG. The coverslips were washed with PBG and incubated with FITC-conjugated goat antimouse antibody (Molecular Probes) in PBG. The percentage of cells displaying an apoptotic phenotype (diffuse cytochrome *c* staining and condensed chromatin) was scored by microscopic investigation. Images were obtained by confocal laser scanning microscopy (LSM 410; Zeiss, Jena, Germany).

Flow Cytometric Apoptosis Assay. Cells were treated for 4 days with the indicated concentration of WK175. The cells were stained by adding 1:1 staining buffer containing 4 μg/ml DAPI (Partec), 20 μg/ml sulforhodamine 101, and 0.1% (v/v) Triton X-100 and analyzed with a particle analyzing system (Partec). Apoptotic cells were detected as the sub-G_1 population on the DNA distribution histogram after DAPI staining.

Inhibition of WK175-induced apoptosis by caspase inhibitors (Calbiochem, Bad Soden, Germany) or bongkrekic acid (Calbiochem) was determined as follows: cells were preincubated for 4 h with 100 μM caspase 1 inhibitor (Ac-YVAD-CHO), caspase 3 inhibitor (Z-DEVD-FMK), and caspase 9 inhibitor (Z-LEHD-FMK) or with 100 μM bongkrekic acid in medium. Then, medium with or without 20 nM WK175 was added to obtain a final concentration of 2×10^5 cells/ml, 50 μM caspase inhibitor or 50 μM bongkrekic acid, and 10 nM WK175. Cells were incubated for an additional 40 h, and the sub-G_1 population was determined on the DNA distribution histogram after DAPI staining.

RESULTS

WK175 Inhibits the Cellular Metabolic Activity of THP-1 Cells and Induces Apoptosis. Treatment of the monocytic leukemia cell line THP-1 with WK175 led to a dose-dependent decrease in metabolic activity, as determined with the WST-1 assay, which is dependent on the dehydrogenase activity and NAD^+ (Fig. 1*A*). An IC_{50} value of 0.2 nM was calculated for WK175 when cells were treated with WK175 for 4 days. The percentage of apoptotic cells, defined as the percentage of cells in the sub-G_1 fraction of the cell cycle, was also determined on day 4. As shown in Fig. 1*B*, a dose-dependent increase was observed in the percentage of apoptotic cells.

Time-dependent Decrease of the Intracellular NAD^+ Content after WK175 Treatment. The concentration of the pyridine nucleotides NAD^+, NADH, $NADP^+$, and NADPH was determined in control and WK175-treated THP-1 cells. As shown in Fig. 2*A*, the intracellular NAD^+ content decreased rapidly after treatment with 10 nM WK175: the concentration was reduced to 27.1% (48 ± 3 pmol $NAD^+/10^6$ WK175-treated cells compared with 178 ± 18 pmol $NAD^+/10^6$ control cells) and 6.7% (17 ± 1 pmol $NAD^+/10^6$ WK175-treated cells compared with 250 ± 30 pmol $NAD^+/10^6$ control cells)

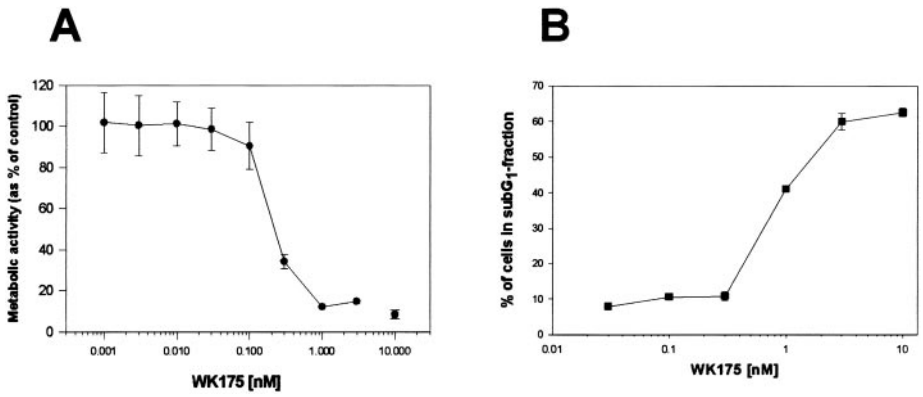

Fig. 1. WK175 causes inhibition of cellular metabolic activity and induces apoptosis in THP-1 cells. *A,* THP-1 cells were treated for 4 days with the indicated concentrations of WK175. The 10 nM data point was determined independently. Cell viability was measured with the WST-1 assay system, which measures the dehydrogenase activity and NAD^+ content of the cells. *B,* THP-1 cells were treated for 4 days with increasing concentrations of WK175 to obtain the dose-response curve. Apoptotic cells were defined as those that appeared as the sub-G_1 population on a DNA distribution histogram.

of the controls after 4 and 12 h of WK175 treatment, respectively. Twenty-four h after the addition of the compound, NAD^+ was undetectable. As shown in Fig. 2*A*, the intracellular NADH, $NADP^+$, and NADPH decrease lagged behind the NAD^+ decrease. After 12 h of WK175 treatment, the intracellular concentrations of NADH, $NADP^+$, and NADPH were 42.5%, 59.3%, and 53.5% of the untreated cells, respectively. Twenty-four h after the addition of WK175, the intracellular NADH concentration decreased to 19.6%, which is 30 ± 1 pmol NADH/10^6 WK175-treated cells compared with 241 ± 23 pmol NADH/10^6 control cells. The concentrations of NADP and NADPH were reduced to 43.6% and 35.5% of the control, respectively. However, because the absolute values of $NADP^+$ and NADPH were lower than those of NAD^+ and NADH, the dramatic decrease in NAD^+ concentration is still reflected in the time-dependent decrease of total intracellular pyridine nucleotide concentration.

WK175 Alters the Mitochondrial Membrane Potential. We measured the effect of WK175 on the mitochondrial membrane potential ($\Delta\Psi_m$) of THP-1 cells in a time course experiment. WK175 (10 nM) was used in the following experiments, representing 50 times the IC_{50} value, as determined by WST-1 assay. The $\Delta\Psi_m$ was measured with the membrane potential-sensitive dye JC-1. JC-1 exists as green fluorescent monomers at low concentrations due to low membrane potential, as in the case of the cytoplasmic membrane potential. The higher potential of the mitochondrial membrane leads to a higher concentration of JC-1 in the mitochondria, resulting in the formation of red fluorescent J-aggregates. Thus, the potential of mitochondria can be monitored by red fluorescence measurements (19).

No change was observed in the amount of cells with high $\Delta\Psi_m$ up to 28 h after treatment with WK175, as shown in Fig. 2*B*. However, 32 h after treatment, the percentage of cells with normal $\Delta\Psi_m$ decreased slightly and continued to decrease until up to 40 h after treatment, at which time point 31% of the cells were left with normal $\Delta\Psi_m$. These results demonstrate that to see an effect on the $\Delta\Psi_m$, the cells need to be exposed to WK175 for more than 28 h.

Release of Cytochrome *c*. Cytochrome *c* is one of the factors released by mitochondria after $\Delta\Psi_m$ disruption. To examine this step in the apoptotic cell death pathway initiated by WK175, cytochrome *c* release was examined in time course studies. THP-1 cells were incubated with 10 nM WK175 and harvested at various time points. The distribution of cytochrome *c* was studied by confocal laser scanning microscopy after immunolabeling cytochrome *c* in whole fixed cells. Cytochrome *c* displayed a dotted pattern, consistent with its location within the mitochondria, in untreated cells (Fig. 3*A*) and in cells treated for 24 h. After 30 h, the staining pattern became more diffuse in 7% of the cells, consistent with a translocation of cytochrome *c* into the cytosol. After 36 h of treatment, this was observed in 23% of the cells, and this number increased to 53% after 42 h (percentages of cells displaying apoptotic phenotype were scored by microscopic investigation of labeled cells). Cells with diffuse cytochrome *c* staining appeared to be apoptotic because in these cells

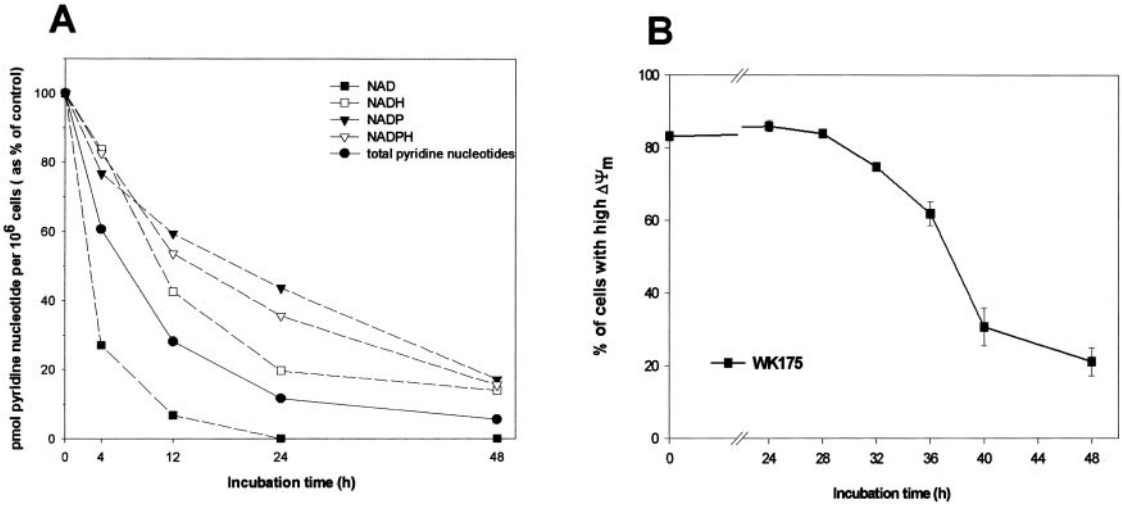

Fig. 2. Effect of WK175 on the steady-state level of intracellular pyridine nucleotides and on the $\Delta\Psi_m$ of THP-1 cells. *A,* THP-1 cells were incubated with 10 nM WK175 and harvested after the indicated time. Cells were lysed, and the pyridine nucleotide content was analyzed as described in "Materials and Methods." The concentration of NAD^+, NADH, $NADP^+$, and NADPH was determined in WK175-treated and untreated control cells at each time point and expressed as a percentage of the control. *B,* THP-1 cells were treated with 10 nM WK175. At the indicated times, fluorescence-activated cell-sorting analysis was performed with the fluorescent dye JC-1 to measure the percentage of cells with high $\Delta\Psi_m$.

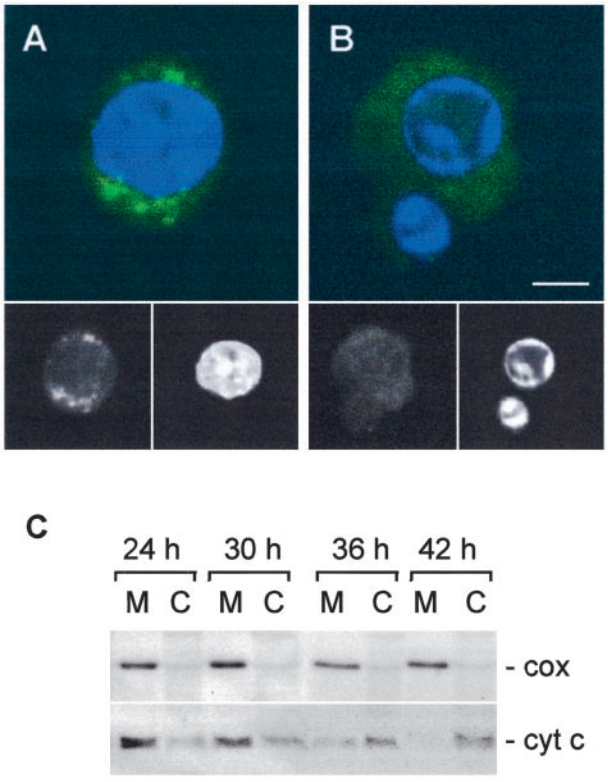

Fig. 3. Effect of WK175 on cytochrome *c* release. Microscopic analysis of cytochrome *c* and DNA-stained THP-1 cells. THP-1 cells treated with control medium **(***A***)** and cells treated for 42 h with 10 nM WK175 **(***B***)** were fixed and labeled for cytochrome *c* (*green*) and DNA (*blue*). Images were obtained with confocal laser scanning microscopy. *Insets* show separate channels. The *bar* represents 5 μm. *C*, THP-1 cells were treated with 10 nM WK175. At the indicated times, the cells were fractionated into mitochondria (*M*) and cytosol (*C*) and assessed for cytochrome *c* (*cyt c*) and cytochrome oxidase (*cox*) by immunoblot.

condensation and margination of the chromatin or, in later stadia, fragmentation of the nucleus was also observed by staining DNA with DAPI (Fig. 3*B*). We also observed that the intensity of cytochrome *c* staining in the apoptotic cells decreased, especially in cells in which the nucleus was already fragmented, possibly due to degradation of cytochrome *c* by proteases or because the cell membrane becomes permeable.

Similar results were observed when cytochrome *c* release from the mitochondria was determined by Western blotting. For this experiment, the cells were fractionated into mitochondria and cytosol. The blot was probed with a cytochrome *c* antibody. To exclude the possibility that mitochondria were disrupted during the fractionation process, resulting in contamination of mitochondrial proteins in the cytosolic fraction, the blot was also probed with a cytochrome oxidase antibody, a protein that resides in the mitochondrial inner membrane. No cytochrome oxidase was observed in the cytosolic fraction (Fig. 3*C*). After 24 h of incubation with WK175, most of the cytochrome *c* was still present in the mitochondria. After 36 h, most of the cytochrome *c* was released into the cytosol, and it was observed that the amount of cytochrome *c* decreased during the apoptotic process. These results are consistent with the timing of the disruption of the $\Delta\Psi_m$. Therefore, we conclude that cytochrome *c* release is part of the apoptosis pathway induced by WK175.

Activation of Caspase 3. To examine the activation of caspase 3 as part of the apoptotic signaling pathway initiated by WK175, the caspase 3 activity of cell extracts was measured in time course studies using the fluorochrome DEVD-AFC as substrate. As shown in Fig. 4*A*, no increase in caspase 3 activity was found after 24 h of incubation with 10 nM WK175. At 30 h, the caspase 3 activity was clearly increased. At 36 h, the activity reached its maximum. This shows that caspase 3 is activated rapidly after disruption of the mitochondrial functions.

Cleavage of Caspase 3 and PARP. The caspase 3 pro-enzyme has a molecular weight of 32,000 and is cleaved during the apoptotic process into three fragments with a molecular weight of 3,000, 12,000, and 17,000, respectively. We examined the cleavage of caspase 3 induced by WK175. THP-1 cells were incubated with 10 nM WK175 and harvested at the times indicated in Fig. 4*B*. No cleavage

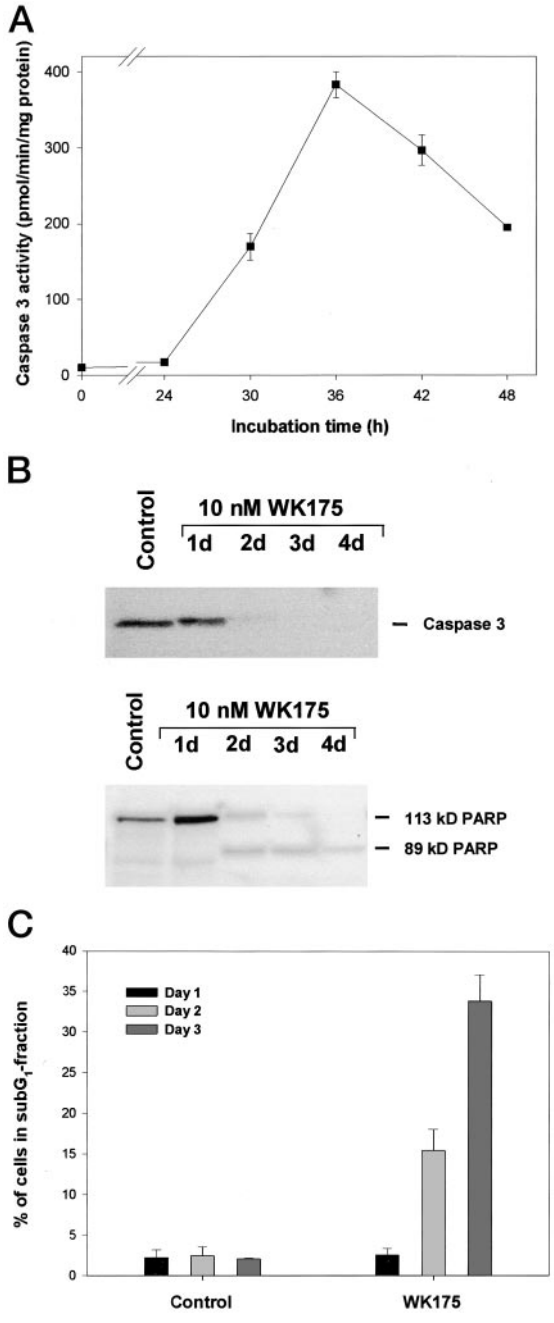

Fig. 4. *A*, effect of WK175 on caspase 3 activity. THP-1 cells were treated with 10 nM WK175. At the indicated times, the cells were extracted and assessed for caspase activity using the fluorochrome DEVD-AFC as substrate. *B*, WK175-induced cleavage of caspase 3 and PARP. THP-1 cells were treated with 10 nM WK175 and harvested after the indicated times. Protein extracts were prepared and analyzed for caspase 3 or PARP cleavage by Western blot. *C*, time-dependent effect of WK175 on the appearance of cells in the sub-G_1 fraction of the cell cycle. THP-1 cells were treated with 10 nM WK175, and cell cycle analysis was performed on days 1, 2, and 3.

of the caspase 3 enzyme was observed 1 day after treatment with WK175. However, a decreased caspase 3 protein signal was observed on days 2, 3, and 4, suggesting cleavage into the active enzyme. These results are consistent with the results of the caspase 3 activity assay (Fig. 4*A*), in which it was demonstrated that caspase 3 activity reaches a maximum 36 h after treatment with WK175.

One of the substrates of caspases is PARP (17). We therefore determined the effect of WK175 on PARP cleavage in a Western blot experiment. As shown in Fig. 4*B*, no PARP cleavage was observed 1 day after treatment with 10 nM WK175. On day 2, cleavage was observed, and some of the M_r 113,000 fragment of PARP was still present. On days 3 and 4, only the M_r 89,000 fragment was observed, and it was observed with decreasing intensity on day 4, probably due to cellular degradation of the cleaved PARP.

Appearance of Cells in the Sub-G_1 Fraction of the Cell Cycle. Deoxyribonucleases, which mediate the internucleosomal cleavage of DNA, are activated during apoptosis (15). Some of the resulting DNA fragments are released during the permeabilization and staining procedures for flow cytometric cell cycle analysis. Thus, apoptotic cells show less DNA staining and appear as a sub-G_1 population on a DNA distribution histogram. The appearance of cells in the sub-G_1 fraction of the cell cycle was measured by flow cytometry on days 1, 2, and 3 after the addition of 10 nM WK175, using SR101 as protein and DAPI as DNA stain (Fig. 4*C*). No increase was observed in the amount of cells in the sub-G_1 fraction 1 day after the addition of WK175 (3%). However, on days 2 and 3, we observed that 15% and 34%, respectively, of the cells treated with WK175 were distributed in the sub-G_1 fraction of the cell cycle. In addition, internucleosomal DNA fragmentation, as indicated by the characteristic "laddering" pattern of DNA separated by electrophoresis on agarose gels, was observed when HL60 cells were treated with 3 or 10 nM WK175 for 2 and 3 days, but not after 1 day of treatment (data not shown). As already observed with the WK175-induced effect on $\Delta\Psi_m$, cytochrome *c* release, caspase activity, and cleavage of caspase 3 and PARP, these results confirm that more than 1 day of WK175 treatment is necessary for the appearance of apoptotic cells and suggest that WK175 requires a certain time period to be effective.

Inhibition of WK175-induced Apoptosis by Caspase 3 and 9 Inhibitors and by Bongkrekic Acid. Peptide-based inhibitors of caspases were designed exclusively for specific caspases, which can be used as tools to identify the caspases involved in the apoptotic pathway. We used three peptide-based caspase inhibitors to investigate their inhibitory effect on WK175-induced apoptosis. Ac-YVAD-CHO is a specific caspase 1 inhibitor, Z-DEVD-FMK is a caspase 3 inhibitor, and Z-LEHD-FMK is a specific caspase 9 inhibitor (20). In addition, we examined the effect of bongkrekic acid on WK175-induced apoptosis. It is known that bongkrekic acid inhibits ATP/ADP transport by stabilizing the ANT in an inactive conformation, thereby reducing the probability of PTP gating and stabilizing the mitochondrial membrane potential. ANT and the VDAC, Bax, cyclophilin D, and the benzodiazepine receptor are thought to come together at the mitochondrial inner and outer membrane contact points to create the PTP (21). The opening of the PTP is associated with the release of cytochrome *c* and AIF and the activation of pro-caspase 9.

THP-1 cells were preincubated for 4 h with the caspase inhibitors or bongkrekic acid before the addition of 10 nM WK175. The cells were then incubated for an additional 40 h and analyzed for the appearance of cells in the sub-G_1 fraction of the cell cycle by flow cytometry. As depicted in Fig. 5, Z-DEVD-FMK and Z-LEHD-FMK inhibited WK175-induced apoptosis to 2.5 ± 0.9% and 4.9 ± 1.2%, respectively, of cells in the sub-G_1 phase of the cell cycle, as compared with 21.2 ± 3.7% of cells in the sub-G_1 phase of the cell cycle in the WK175-treated population that was not preincubated. In contrast, no inhibitory effect of Ac-YVAD-CHO was observed. These results suggest that caspase 3 and 9 play more important roles in the WK175-induced apoptotic cascade than caspase 1. Bongkrekic acid inhibited WK175-induced apoptosis less potently than Z-DEVD-FMK and Z-LEHD-FMK: the percentage of cells in the sub-G_1 fraction was reduced to 9.0 ± 2.1%.

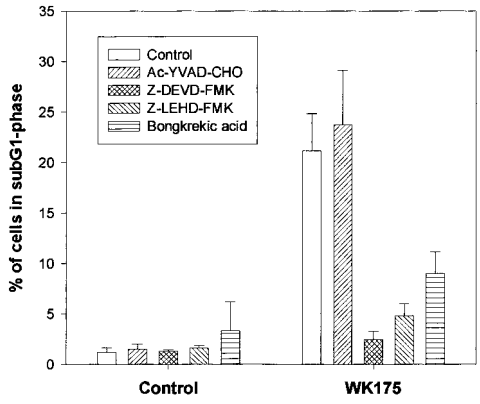

Fig. 5. Inhibition of the WK175-induced effect by caspase inhibitors and bongkrekic acid. THP-1 cells were preincubated with 50 μM caspase inhibitor or 50 μM bongkrekic acid before the addition of 10 nM WK175. The cell cycle distribution was analyzed 40 h after the addition of WK175.

DISCUSSION

We have demonstrated that WK175 is a potent activator of the apoptotic pathway, with distinct characteristics of conventional chemotherapy. WK175 has no DNA-damaging effect and does not alter p53 or p21 expression, like many other apoptosis-inducing drugs do (results not shown). Instead, WK175 interferes with the steady-state level of intracellular NAD^+, resulting in a decreased intracellular NAD^+ concentration. This decreased NAD^+ concentration is the trigger to directly or indirectly activate the apoptotic cascade. Apoptotic events, such as the disruption of the mitochondrial membrane potential, release of cytochrome *c*, activation of caspase 3, cleavage of caspase 3 and PARP, and appearance of apoptotic cells, were observed. To our knowledge, this is the first report that inhibition of NAD^+ metabolism, leading to a decreased NAD^+ concentration, triggers apoptosis.

These apoptotic events were activated 28 h after the addition of WK175, whereas the onset of the decrease in NAD^+ concentration was already observed 2 h after the addition of WK175 in THP-1 cells,[4] suggesting that there is a certain lag period between the primary effect (onset of the decrease in NAD^+ concentration) and the activation of apoptosis. A dramatic reduction of the intracellular NAD^+ content after WK175 treatment was observed: 12 h after the addition of the compound, the NAD^+ content was reduced to 6.7% of the control (Fig. 2*A*). No NAD^+ was detectable after 24 h of WK175 treatment. The lag period between the onset of NAD^+ decrease and cell death was not only observed in THP-1 cells: a lag period was also found in human hepatocarcinoma HepG2 cells and in chronic myelogenous leukemia K562 cells (results not shown). Our hypothesis is that the NAD^+ concentration has to reach a minimal concentration to trigger the induction of cell death. It is also possible that a rapid decrease in cytosolic NAD^+ takes place, whereas the NAD^+ concentration in the mitochondria is relatively unaffected, and that the mitochondrial NAD^+ concentration is also reduced only after a certain time period. This NAD^+ reduction could then limit the metabolic functions of the mitochondria, which subsequently gives rise to the activation of apoptosis. Therefore, apoptotic events, such as disruption

of membrane potential, cytochrome *c* release, and caspase activation, are seen relatively late (28–42 h after the addition of WK175) in comparison with the early apoptosis induction seen with some DNA-damaging compounds. A decrease in NAD^+ levels has been described with cytotoxic agents that was attributed to DNA damage-induced PARP activation (22–24). However, this effect is distinct from the WK175-induced NAD^+ decrease in that the time between NAD^+ decrease and cell death does not exceed a few hours.

NAD^+ has important roles in metabolic functions of the cell. For example, NAD^+ is involved in the glycolysis pathway, the citric acid cycle generating ATP, and the oxidative phosphorylation in which electron transfer to NAD^+ and from NADH takes place. NAD^+ is recycled in these reactions, which is in contrast to reactions that consume NAD^+. NAD^+ is consumed as a substrate by the NAD-catabolizing enzymes [ADP-ribosyltransferases (like PARP)], NAD-glycohydrolases, and ADP-ribosyl cyclase (25–27). Our results indicate that during WK175 treatment, cellular NAD^+ decreased more dramatically and more rapidly than NADH, $NADP^+$, and NADPH, respectively. This observation is well in line with previous reports that describe NAD^+ to be the preferred substrate of the NAD-cleaving enzymes (26, 28).

It was described that NADH and NADPH induced closure of the VDAC when reconstituted into phospholipid membranes, with NADH being five times more potent (29). The VDAC on the outer membrane and the ANT on the inner membrane of the mitochondria are the principle mediators of adenine nucleotide exchange between the matrix and the cytosol (21). It was shown that mitochondrial outer membrane permeability is subject to regulation by growth factor withdrawal and the activity of the antiapoptotic proteins Bcl-x_L and Bcl-2 (30). Interleukin 3 withdrawal resulted in closure of the VDAC, which is prevented by the outer mitochondrial membrane proteins Bcl-x_L and Bcl-2. The authors suggested that Bcl-x_L and Bcl-2 function to maintain VDAC in an open configuration to promote cell survival. Whether the decreased NAD^+ concentration and concomitantly decreased NADH and NADPH concentration observed after WK175 treatment trigger apoptosis through VDAC permeability changes or whether WK175 itself induces VDAC permeability changes that result in the induction of apoptosis is currently under investigation.

Inhibition of WK175-induced apoptosis was observed with bongkrekic acid, Z-DEVD-FMK, and Z-LEHD-FMK. Bongkrekic acid stabilizes the mitochondrial membrane potential, whereas Z-DEVD-FMK and Z-LEHD-FMK prevented caspase 9 and 3 activation, thereby inhibiting the effect of WK175 on apoptosis. Other specific apoptosis inhibitors are expected to interfere with WK175-induced cell death as well. For example, we observed that Bcl-2-overexpressing MDA-MB-231 cells displayed a reduced sensitivity to WK175 (results not shown).

WK175 has been tested in xenograft models in nude mice using tumors from the breast, bladder, prostate, lung, colon, and liver and shown significant tumor growth inhibition (data not shown), making WK175 a promising antitumor drug candidate acting by a new mechanism.

All things considered, the present study demonstrates that WK175 is a novel antitumor agent that decreases the intracellular NAD^+ concentration, which results in the activation of the apoptotic cascade, in which the dissipation of the mitochondrial membrane potential, cytochrome *c* release, and caspase activation are involved.

REFERENCES

1. Kroemer, G. The proto-oncogene Bcl-2 and its role in regulating apoptosis. Nat. Med., *3:* 614–620, 1997.
2. Jacobson, M. D., Weil, M., and Raff, M. C. Programmed cell death in animal development. Cell, *88:* 347–354, 1997.
3. Barinaga, M. Death by a dozen of cuts. Science (Wash. DC), *280:* 32–34, 1998.
4. Costantini, P., Jacotot, E., Decaudin, D., and Kroemer, G. Mitochondria as a novel target of anticancer chemotherapy. J. Natl. Cancer Inst. (Bethesda), *92:* 1042–1053, 2000.
5. Marchetti, P., Castedo, M., Susin, S. A., Zamzami, N., Hirsch, T., Macho, A., Haeffner, A., Hirsch, F., Geuskens, M., and Kroemer, G. Mitochondrial permeability transition is a central coordinating event of apoptosis. J. Exp. Med., *184:* 1155–1160, 1996.
6. Kantrow, S. P., and Piantadosi, C. A. Release of cytochrome *c* from liver mitochondria during permeability transition. Biochem. Biophys. Res. Commun., *232:* 669–671, 1997.
7. Susin, S. A., Zamzami, N., Castedo, M., Hirsch, T., Marchetti, P., Macho, A., Daugas, M., Geuskens, M., and Kroemer, G. Bcl-2 inhibits the mitochondrial release of an apoptotic protease. J. Exp. Med., *184:* 1331–1342, 1996.
8. Du, C., Fang, M., Li, Y., Li, L., and Wang, X. Smac, a mitochondrial protein that promotes cytochrome *c*-dependent caspase activation by eliminating IAP inhibition. Cell, *102:* 33–42, 2000.
9. Verhagen, A. M., Ekert, P. G., Pakusch, M., Silke, J., Connolly, L. M., Reid, G. E., Moritz, R. L., Simpson, R. J., and Vaux, D. L. Identification of DIABLO, a mammalian protein that promotes apoptosis by binding to and antagonizing inhibitor of apoptosis (IAP) proteins. Cell, *102:* 43–53, 2000.
10. Liu, S., Kim, C. N., Yang, J., Jemmerson, R., and Wang, X. Induction of apoptotic program in cell-free extracts: requirement for dATP and cytochrome *c*. Cell, *86:* 147–157, 1996.
11. Susin, S. A., Lorenzo, H. K., Zamzami, N., Marzo, I., Snow, B. E., Brothers, G. M., Mangion, J., Jacotot, E., Costantini, P., Loeffler, M., Narochette, N., Goodlett, D. R., Aebersold, R., Siderovski, D. P., Penninger, J. M., and Kroemer, G. Molecular characterization of mitochondrial apoptosis-inducing factor. Nature (Lond.), *397:* 441–446, 1999.
12. Li, P., Nijhawan, D., Budihardjo, I., Srinivasula, S. M., Ahmad, M., Alnemri, E. S., and Wang, X. Cytochrome *c* and dATP-dependent formation of Apaf-1/caspase-9 complex initiates an apoptotic protease cascade. Cell, *91:* 479–489, 1997.
13. Zou, H., Li, Y., Liu, X., and Wang, X. An Apaf-1/cytochrome *c* multimeric complex is a functional apoptosome that activates procaspase-9. J. Biol. Chem., *274:* 11549–11556, 1999.
14. Hu, Y., Benedict, M. A., Ding, L., and Nunez, G. Role of cytochrome *c* and dATP/ATP hydrolysis in Apaf-1-mediated caspase-9 activation and apoptosis. EMBO J., *18:* 3586–3595, 1999.
15. Enari, M., Sakahari, H., Yokoyama, H., Okawa, K., Iwamatsu, A., and Nagata, S. A caspase-activated DNase that degrades DNA during apoptosis, and its inhibitor ICAD. Nature (Lond.), *391:* 43–50, 1998.
16. Kothakota, S., Azuma, T., Reinhard, C., Klippel, A., Tang, J., Chu, K., McGarry, T. J., Kirschner, M. W., Koth, K., Kwiatkoski, D. J., and Willams, L. T. Caspase-3-generated fragment of gelsolin: effector of morphological change in apoptosis. Science (Wash. DC), *278:* 294–297, 1997.
17. Nicholson, D. W., Ambereen, A., Thornberry, N. A., Vaillancourt, J. P., Ding, C. K., Gallant, M., Gareau, Y., Griffing, P. R., Labelle, M., Lazebnik, Y. A., Munday, N. A., Raju, S. M., Smulson, M. E., Yamin, T., Yu, V. L., and Miller, D. K. Identification and inhibition of the CED-3 protease necessary for mammalian apoptosis. Nature (Lond.), *376:* 37–43, 1995.
18. Pinder, S., Clark, J. B., Greenbaum, A. L. The assay of intermediates and enzymes involved in the synthesis of nicotinamide nucleotides in mammalian tissues. Methods in Enzymology, *18B:* 20–46, 1971.
19. Salvioli, S., Ardizzoni, A., Franceschi, C., and Cossarrizza, A. JC-1, but not DiOC6(3) or rhodamine 123, is a reliable fluorescent probe to assess $\Delta\Psi$ changes in intact cells: implications for studies on mitochondrial functionality during apoptosis. FEBS Lett., *411:* 77–82, 1997.
20. Thornberry, N. A., Rosen, A., and Nicholson, D. W. Control of apoptosis. Adv. Pharmacol., *41:* 155–177, 1997.
21. Wallace, D. C. Mitochondrial diseases in man and mouse. Science (Wash. DC), *283:* 1482–1488, 1999.
22. Komatsu, N., Nakagawa, M., Oda, T., and Muramatsu, T. Depletion of intracellular NAD^+ and ATP levels during ricin-induced apoptosis through the specific ribosomal inactivation results in the cytolysis of U937 cells. J. Biochem., *128:* 463–470, 2000.
23. Petitt, A. R., Sherrington, P. D., and Cawley, J. C. Role of poly(ADP-ribosyl)ation in the killing of chronic lymphocytic leukemia cells by purine analogues. Cancer Res., *60:* 4187–4193, 2000.
24. Sims, J. L., Berger, S. J., and Berger, N. A. Poly(ADP-ribose) polymerase inhibitors preserve nicotinamide adenine dinucleotide and adenosine 5′-triphosphate pools in DNA-damaged cells: mechanism of stimulation of unscheduled DNA synthesis. Biochemistry, *22:* 5188–5194, 1983.
25. Wielckens, K., Schmidt, A., George, E., Bredehorst, R., and Hilz, H. DNA fragmentation and NAD depletion. Their relation to the turnover of endogenous mono(ADP-ribosyl) and poly(ADP-ribosyl) proteins. J. Biol. Chem., *257:* 12872–12877, 1982.
26. Price, S. R., and Pekala, P. H. Pyridine nucleotide-linked glycohydrolases. *In:* D. Dolphin, R. Poulson, and O. Avramovic (eds.), Pyridine Nucleotide Coenzymes: Chemical, Biological and Medical Aspects, pp. 513–548. New York: Wiley-Interscience, 1987.
27. Lee, H. C., and Aarhus, R. ADP-ribosyl cyclase: an enzyme that cyclizes NAD^+ into a calcium-mobilizing metabolite. Cell Regul., *2:* 193–203, 1991.
28. Cory, J. Purine and pyrimidine nucleotide metabolism. *In:* T. Devlin (ed.), Textbook of Biochemistry with Clinical Correlations, 3rd ed., pp. 529–574. Brisbane, Australia: Wiley, 1992.
29. Colombini, M., Bachly-Dyson, E., and Forte, M. VDAC, a channel in the outer mitochondrial membrane. *In:* T. Narahashi (ed.), Ion Channels, Vol. 4, pp. 169–202. New York: Plenum Publishing Corp., 1996.
30. Vander Heiden, M. G., Chandel, N. S., Xian Li, X., Schumacker, P. T., Colombini, M., and Thompson, C. B. Outer mitochondrial membrane permeability can regulate coupled respiration and cell survival. Proc. Natl. Acad. Sci. USA, *97:* 4666–4671, 2000.

WK175, a Novel Antitumor Agent, Decreases the Intracellular Nicotinamide Adenine Dinucleotide Concentration and Induces the Apoptotic Cascade in Human Leukemia Cells

Katja Wosikowski, Karin Mattern, Isabel Schemainda, et al.

Cancer Res 2002;62:1057-1062.